Impact of Lateral Doping Profiles on Ultra-scaled Trigate FinFETs

R. Valin, M. Aldegunde, A. Martinez, and J. R. Barker*
College of Engineering, Swansea University, UK
*School of Engineering, University of Glasgow, G12 9YH, UK
e-mail: r.valinferreiro@swansea.ac.uk

The implementation of lateral doping profiles on quantum transport simulations of ultra–scaled transistors will affect the tunneling current. This work presents a systematic study of the impact of lateral doping profiles when the gate length of silicon Trigate FinFETs is scaled down from 6.6nm to 5.4nm [1]. We use the Non-equilibrium Green's Functions (NEGF) method for ballistic and dissipative transport (phonon scattering). The cross section of both devices is kept constant with silicon thickness at 4.2nm and fin–height at 10.6nm. The equivalent oxide thickness of the gate is 0.48nm. The channel region is undoped and the length of source and drain regions are each 10nm. To simulate the impact of the lateral doping, a Gaussian doping profile has been considered such as is shown in Fig. 1 [2]. The current characteristics of the 6.6nm FinFET at V_D=0.7V, depicted in Fig. 2, show important differences in the sub–threshold region between the Gaussian doping (squared points) and the abrupt doping (rounded points), with an 18% larger value of the sub–threshold slope for the abrupt doping regarding the Gaussian doping. Fig. 2 also shows that the 6.6nm FinFET in the sub–threshold region is working in the ballistic regime, regardless of the doping profile, since the ballistic (red lines) and phonon scattering (black lines) simulations are overlapped for the Gaussian and abrupt doping profiles. In addition, for the saturation region the current dissipation due to phonon scattering can be evaluated for the Gaussian and abrupt doping profiles to be 27% and 19% respectively. The ballistic regime can also be observed when the gate length is scaled down to 5.4nm. Fig. 3 shows the ballistic and dissipative (phonon scattering) currents are overlapped for both doping profiles. For the 5.4nm gate length FinFET, the differences in the sub–threshold regions are larger, since the sub–threshold slope of the abrupt doping profile at V_D=0.7V is 30% larger than the value of the Gaussian doping profile. Fig. 2 and Fig. 3 show that the Gaussian doping profile improves the sub–threshold slope of the device, reducing the saturation current to around a 30% of the value obtained with the abrupt doping profile. A degradation of the sub–threshold slope when the gate length is shrunk is also observed from a comparison of the current characteristics between the 5.5nm and 6.6nm FinFET with Gaussian doping profiles shown in Fig. 4. However, the current reduction in the saturation region due to the the phonon scattering is a 10% smaller for the 5.4 nm. Fig. 4 shows that the FinFET with smaller gate length has a larger off–current since the tunneling current probability is larger with smaller widths of the barrier. Fig. 5 shows the bands along the transport direction for both devices, 5.4nm (blue lines) and 6.6nm (red lines) at V_G=0.3V. The bands for the Gaussian (triangular symbols) and abrupt (squared symbols) doping profiles show a larger effect of the DIBL on the 5.4nm FinFET device, decreasing the height of the barrier and consequently increasing the off–current. We conclude that the Gaussian doping profile increases the effective channel length which reduces the DIBL effect and improves the control over the channel. This effect can be observed in Fig. 6 where the iso–surfaces of the electron concentration show higher concentrations of electrons in the channel region for the abrupt doping at V_G=0.3V.

REFERENCES

[1] ITRS. International Roadmap for the Semiconductor Industry, Update, (2012).

[2] Vishal P. Trivedi et al. Nanoscale FinFETs With Gate-Source/Drain Underlap. *IEEE Transactions on Electron Devices*, 52:56–62, (2005).

ISBN 978-2-9547858-0-6

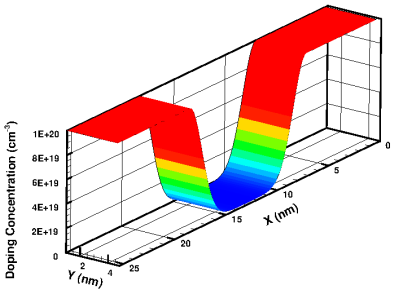

Fig. 1: Gaussian doping profile ($N_{SD} \propto e^{(\frac{x-x_0}{\sigma_L})^2}$) of 5.4nm Trigate FinFET, $N_{SD} = 10^{20} cm^{-3}$, $\sigma_L =$ 1.73nm, $x_0(source) =$ 7nm and $x_0(drain) =$ 18.4nm. The Gaussian doping profile has been scaled according to the scaling of the gate length for the 6.6nm Trigate FinFET, $\sigma_L =$ 2.11nm, $x_0(source) = 6.4$nm and $x_0(drain) = 20.2$nm.

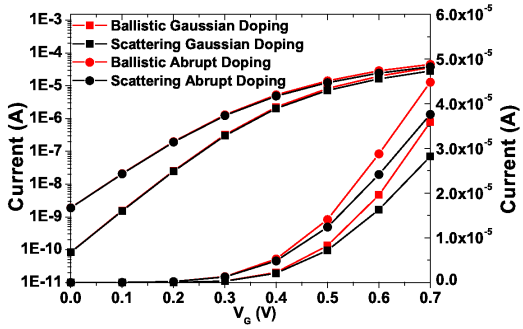

Fig. 2: Current characteristics of the 6.6nm gate length Trigate FinFET with Gaussian and abrupt doping at V$_D$= 0.7V for ballistic transport and phonon scattering.

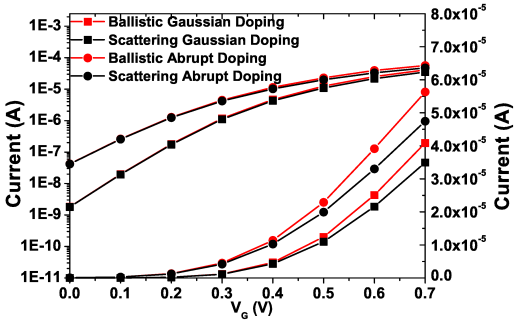

Fig. 3: Current characteristics of the 5.4nm gate length Trigate FinFET with Gaussian and abrupt doping at V$_D$= 0.7V for ballistic transport and phonon scattering.

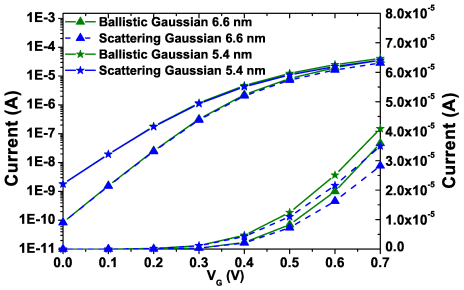

Fig. 4: Comparison of current characteristics between 5.4nm gate length and 6.6nm gate length Trigate FinFETs with equivalent Gaussian doping at V$_D$= 0.7V for ballistic transport and phonon scattering.

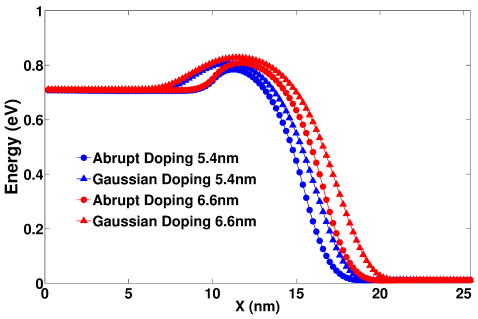

Fig. 5: Immpact of Gaussian and abrupt doping on the first subband of 5.4nm gate length and 6.6nm gate length Trigate FinFETs with Gaussian and abrupt doping at V$_D$= 0.7V and V$_G$= 0.3V.

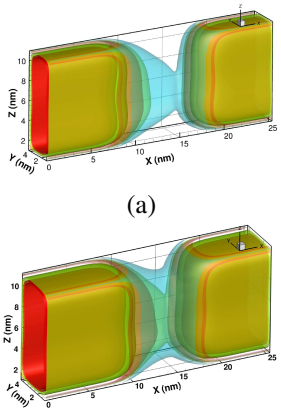

(a)

(b)

Fig. 6: Isosurfaces of the electron distribution of the 5.4nm gate length Trigate FinFET with (a) Gaussian and (b) abrupt doping profiles at V$_G$= 0.3V.